populated, and their contribution to the tunneling is usually neglected. In Refs [16, 17], an effect of successive resonance tunneling over the excited states in long-period superlattices was found, which was accompanied by the appearance of resonance features in current – voltage multistability branches. These experiments demonstrate the existence of a new type of the electric field domain with the excited-to-excited states resonance in neighboring quantum wells. The results of these studies also lead to a fundamental conclusion about the strongly nonequilibrium distribution of charge carriers in lower subbands with energies less than the optical phonon energy [16, 17], in accordance with the measurements of radiation at the intersubband transitions in analogous superlattices [11].

Conclusions

We considered the problem of the development of lasers of a new type operating on intersubband transitions using resonance tunneling in quantum-sized semiconductor structures with wide quantum wells. The results of investigation of resonance tunneling in an electric field in long-period superlattices and structures with wide quantum wells are presented. It was shown experimentally that the resonance tunneling in these structures could lead to efficient and selective depopulation of the levels, resulting in a population inversion for charge carriers in lower subbands. The important role of the spatial charge was shown in processes resulting in the mismatch of the resonance levels and transformation of the resonance tunneling structure itself in an electric field. Based on these studies, a conclusion is made about the structure and structural parameters which are the most promising for producing a population inversion and stimulated radiation at the intersubband transitions in systems with wide quantum wells.

Acknowledgements
This work was supported by the State Scientific and Technical Programs "Physics of solid-state nanostructures" (project 97-1048) and "Perspective technologies and devices in micro- and nanoelectronics" (project 133/57/2) and the Russian Foundation for Basic Research (grant 97-2-17474).

References

1. Andronov A A et al. *Submillimetrovye Lazery na Goryachikh Dyrkakh v Poluprovodnikakh* (Submillimeter Lasers on Hot Holes in Semiconductors) (Ed. A A Andronov) (Gor'kiĭ: Izd. Inst. Prikl. Fiz. Akad. Nauk SSSR, 1986)
2. Allen S J et al. *Semicond. Sci. Technol.* **7** B1 (1992)
3. Andronov A *Semicond. Sci. Technol.* **7** B629 (1992)
4. Kazarinov R F, Suris R A *Fiz. Tekh. Poluprovodn.* **5** 797 (1971) [*Sov. Phys. Semicond.* **5** 707 (1971)]
5. Faist J et al. *Science* **264** 553 (1994)
6. Gauthier-Lafaye O et al. *Appl. Phys. Lett.* **71** 3619 (1997)
7. Ferreira R, Bastard G *Phys. Rev.* **40** 1074 (1989)
8. Haberle A P et al. *Semicond. Sci. Technol.* **9** 519 (1994)
9. Stoklitskiĭ S A et al. *Pis'ma Zh. Eksp. Teor. Fiz.* **61** 399 (1995) [*JETP Lett.* **61** 405 (1995)]
10. Mityagin Yu A, Murzin V N *Pis'ma Zh. Eksp. Teor. Fiz.* **64** (3) 146 (1996) [*JETP Lett.* **64** 155 (1996)]
11. Helm M et al. *Phys. Rev. Lett.* **63** 74 (1989)
12. Grahn H T, Schneider H, von Klitzing K *Phys. Rev. B* **41** 2890 (1990)
13. Pregnel F, Wacker A, Scholl E *Phys. Rev. B* **50** 1705 (1994)
14. Rasulova G K et al. *Proc. Int. Symp. "Nanostructures: Physics and Technology", St. Petersburg, Russia* (1995) p. 151; *J. Appl. Phys.* **82** 3381 (1997)
15. Stoklitskiĭ S A et al., in *Tezisy Dokladov Rossiĭskoĭ Konferentsii "Mikroelektronika 94"* (Russian Conference "Microelectronics 94") (Zvenigorod, 1994) (Moscow: Izd. RAN, 1994) p. 97
16. Mityagin Yu A et al. *Pis'ma Zh. Eksp. Teor. Fiz.* **65** 818 (1997) [*JETP Lett.* **65** 852 (1997)]
17. Mityagin Yu A et al. *Appl. Phys. Lett.* **70** 3008 (1997)

PACS numbers: **42.60.–v**, 42.60.By

Blue-green lasers based on short-period superlattices in II – VI compounds

S V Ivanov, P S Kop'ev, A A Toropov

Introduction

Heterostructures based on wide-gap II – VI compound semiconductors (Fig. 1a) still remain the most promising candidates for the development of commercial green laser diodes needed for the laser projection TV and other laser applications requiring laser radiation tunable over the entire visible spectral range. Despite recent attempts to optimize laser diodes with quantum wells (QWs) based on ZnSe, only a slight increase in their life has been achieved so far [1, 2]. Rapid degradation of the laser structures is mainly caused by the nonradiative recombination at defects in the active region [2], resulting in the formation and development of new defects due to the extremely low energy of defect formation, which is typical for most wide-gap II – VI compounds [3].

In this paper, we suggest a new concept for the active region of the II – VI laser structures with the aim of increasing their lifetime. The basic principles of our concept are: (1) The protection of the active medium from the penetration and development of extended and point defects and (2) the spatial separation of defects and sites of radiative recombination of charge carriers directly in the active region. The first problem is solved by introducing a waveguide based on an alternately strained (Zn, Cd)Se/ZnSSe (or BeZnSe/ZnSe) short-period superlattice (SL) in ZnMg(Be or S)Se/ZnCdSe DHS lasers with separate confinement (DHS SC) (Fig. 1b), which results simultaneously in the improvement of the electronic and optical confinement. The replacement of the QW in the recombination region by a CdSe fractional monolayer (FM) insert of thickness 2 – 3 monolayers (ML) in ZnSe solves the second problem due to transformation of the CdSe FM under certain molecular-beam epitaxy (MBE) conditions to a set of self-organizing CdSe-enriched nanoislands, which strongly suppress migration of nonequilibrium carriers towards defects (Fig. 1c). It is also expected that the use of Be chalcogenides, which possess the maximum hardness among all of the II – VI compounds, will result in an increase in the activation energy of formation and development of defects [3, 4].

Experimental

To study the properties of the active region we suggest that optically pumped (Zn, Mg)(S, Se) DHS SC lasers were grown by MBE on GaAs(001) substrates. Also, (Be, Mg, Zn)Se laser diodes with an SL waveguide and two types of recombination regions (the ZnCdSe QW and CdSe FM) were manufactured.

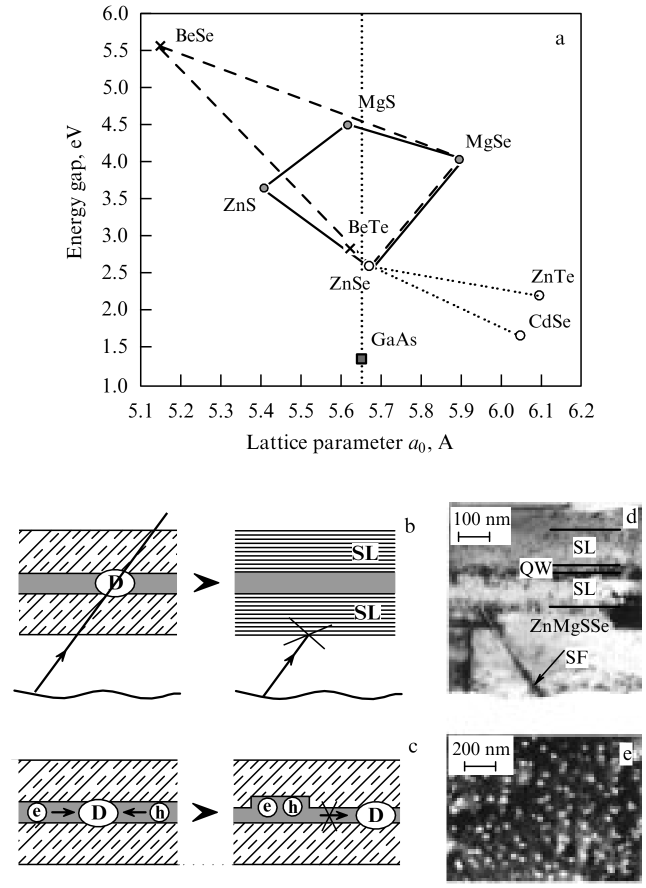

Figure 1. (a) Dependence of the energy gap on the lattice parameter for binary II – VI compounds used in the laser structures under study; (b) and (c) basic elements of a new concept for the active region of degradation stable blue-green II – VI lasers; (d) TEM image of the cross-section of a structure with a ZnSSe/ZnCdSe SL waveguide (SF is the stacking fault defect); (e) plan-view TEM image of the active region of a laser with a 2.8-ML CdSe/ZnSe FM nanostructure.

The parameters of MBE growth and methods for controlling the compositions of S- and Be-containing compounds are described in detail in Refs [5 – 7].

The optically-pumped DHS SL QW structures consisted of lower and upper $Zn_{0.9}Mg_{0.1}S_{0.15}Se_{0.85}$ cladding layers of thickness 0.5 and 0.1 μm, respectively, and the symmetric $ZnS_{0.14}Se_{0.86}$/(Zn, Cd)Se SL waveguide lattice-matched to GaAs with a single 7-nm ZnCdSe QW in the middle. The molar fraction of CdSe in the QW and SL was varied from 0 to 0.27, which allowed coverage of the wavelength range from 470 to 523 nm. The active region of the FM laser represented a separate 5-nm ZnSe/2.8 ML-CdSe/5-nm ZnSe nanostructure surrounded by the 3-nm $ZnS_{0.14}Se_{0.86}$/5-nm-ZnSe SL from both sides. The active region of the BeMgZnSe/ZnCdSe laser diodes consisted of a (1-nm $Be_{0.05}Zn_{0.95}Se$/1.5-nm-ZnSe$)_{82}$ SL waveguide with a 4-nm $Zn_{0.63}Cd_{0.47}Se$ QW or a 2.6 ML-CdSe/ZnSe FM structure at the center. The BeMgZnSe/ZnCdSe laser diodes also contained wide-gap $Be_{0.05}Mg_{0.06}Zn_{0.89}Se$ emitters of n and p types of thickness 1 μm doped with iodine and nitrogen, respectively, and a modulation-doped short-period ZnSe/BeTe SL with a variable step and upper, heavily p-doped contact 10-nm BeTe:N/30-nm ZnTe:N layers. The peculiarities of MBE of the CdSe FM active region are described in detail in Ref. [8].

Structural studies were performed by transmission electron microscopy (TEM) and X-ray diffraction (XRD). Optical and transport properties of the structures were studied by steady-state photoluminescence (PL) and time-resolved PL with a time resolution of 20 ps. The laser parameters were studied upon excitation by a 8-ns nitrogen laser. The structure of injection laser diodes with stripe contacts were studied by the method of standard photolithography and measured as in Ref. [9].

Short-period alternately strained superlattices

The principles of the design, specific features of the growth and basic properties of structures with alternately strained SLs and multiple QWs (MQW) based on II – VI compounds were described earlier [10, 11]. In particular, it was shown [10] that alternately strained ZnSSe/ZnCdSe SL and MQWs have a larger critical thickness compared to the bulk layers with the same lattice mismatch, with their critical thickness even exceeding theoretical estimates of the critical thickness for the average lattice parameter of the SL and MQW. The TEM image of the cross section of the structure of the DHS SC QW laser with the SL (Fig. 1d) demonstrates the possibilities of such SLs for the protection of the active region from penetration of stacking fault defects. Threshold power densities of lasers with the SL waveguide ($P_{\text{thresh}} < 20\,\text{kW cm}^{-2}$) measured over a broad range of lasing wavelengths (490 – 523 nm) at 300 K are among the lowest reported earlier for the II – VI lasers with QW, which suggests that the electronic confinement for holes increased at the optimum optical confinement [12], while the concentration of centers of nonradiative recombination in the QW restricted by the SL decreased. Note that earlier we used the short-period SL waveguide for manufacturing low-threshold (Al, Ga)As DHS SC QW injection lasers [13].

Despite the small width of the lower miniband of heavy holes (hh) in the ZnSe-based SL ($\sim$ 10 meV) because of the large effective mass ($0.6m_0$), efficient transport of charge carriers is observed in such SLs along the SL axis , which is confirmed by measurements of low-temperature steady-state and time-resolved PL spectra [14, 15]. Calculations of the band structure over a broad range of parameters of the ZnSSe/ZnCdSe SL (the numbers of wells and barriers and their widths) showed that the energy gap between the top of the lower hh miniband and the bottom of the much wider (30 – 100 meV) miniband of light holes (lh) does not exceed 10 – 15 meV. This provides efficient occupation of the lh states with increasing temperature, resulting in an efficient thermally activated transfer of holes along the growth axis followed by their subsequent capture onto QWs and energy relaxation to the lower hh levels of QWs.

The concept of the SL waveguide was successfully applied in the BeMgZnSe/ZnCdSe DHS SC QW injection lasers operating at room temperature by using alternately strained BeZnSe/ZnSe SLs surrounding a deep ZnCdSe QW. These lasers demonstrate typical threshold current densities of about $J_{\text{thresh}} = 750\,\text{A cm}^{-2}$ (the minimum value is approximately 450 A cm^{-2}) and the cut-off voltage 7 V, which are determined by insufficiently optimum both p-doping of wide-gap claddings and optical confinement. The lasing spectra of the BeMgZnSe DHS SL QW laser diode are presented in Fig. 2a (the insert). The substantial improvement of the electronic confinement of holes by the SL waveguide results in an increase in the characteristic temperature almost by a factor

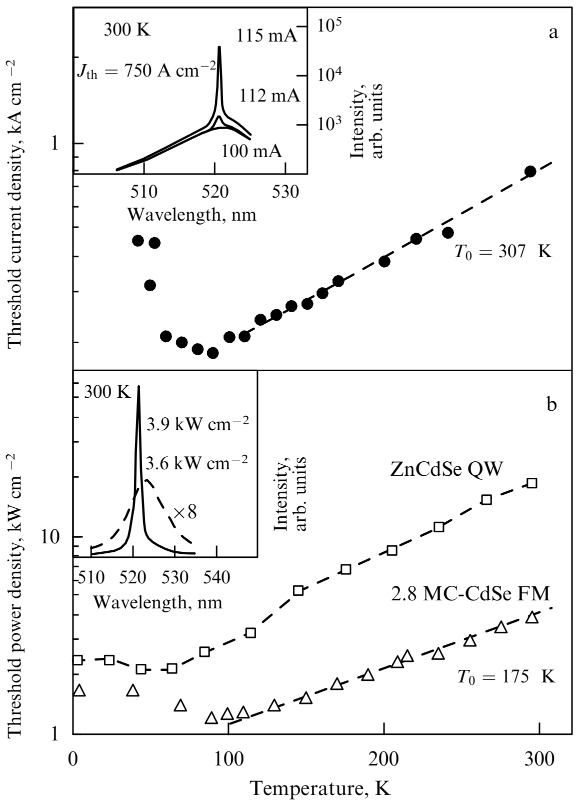

Figure 2. (a) Temperature dependence of the threshold current density for a BeMgZnSe DHS SL QW laser diode. The insert shows lasing spectra at 300 K. (b) Temperature dependences of the threshold power of ZnMgSSe laser structures with FM (triangles) and QW (squares) active regions. The insert shows lasing spectra of the FM structure at 300 K.

of two (up to $T_0 = 307$ K at 300 K) compared to $T_0 \sim 160$ K, which is typical for structures with a bulk BeZnSe waveguide. Figure 2a shows the temperature dependence of the threshold current density for the DHS SL QW laser diode. For temperatures below 80 K, J_{thresh} decreases with increasing temperature, which indicates the validity of the model of thermally activated transport of charge carriers in Be-containing SLs. Note that in buried-stripe laser diodes with a stripe width of 1 μm, the characteristic temperature increased to $T_0 = 340$ K at temperatures above room temperature, which provided the possibility of pulsed laser generation at a maximum temperature of 140 °C [16]. The values given above are maximum among those reported earlier for the II – VI laser diodes.

The CdSe/ZnSe fractional multilayer active region

It was found recently that single CdSe/ZnSe FM structures exhibit bright excitonic PL, which has a maximum intensity near the critical thickness of the CdSe layer (~ 3 MLs) [17]. The dependence of morphology and optical properties of single CdSe/ZnSe FM nanostructures on the nominal thickness w of the CdSe layer varying from 0.1 to 3.6 MLs was studied by the methods of TEM, XRD, PL, and time-resolved PL [8, 18 – 20]. The plan-view TEM image of the single 2.8-ML CdSe/ZnSe FM structure (Fig. 1e) exhibiting the maximum intensity of the integrated PL demonstrates the formation of CdSe-containing self-organizing islands with lateral dimensions 15 – 30 nm and a density of 2×10^{10} cm^{-2}. Large islands (> 30 nm) relaxed with the formation of distinctly oriented defects, however, their density was only 15% of the total density of the islands, whereas 85% of the islands were, probably, pseudomorphic. Note that no structural defects were found outside large islands. We believe that these islands are too large to be electronic quantum dots and rather represent extended regions of ultranarrow QWs with a specific localization potential of charge carriers caused by local fluctuations of the Cd content.

The parameters of a ZnMgSSe laser with a 2.8-ML CdSe FM active region are presented in Fig. 2b. The laser demonstrates the threshold power density at 300 K (less than $P_{thresh} = 4$ kW cm^{-2} at $\lambda \sim 523$ nm) that is less by a factor of five (being minimum among the known values) than $P_{thresh} = 19$ kW cm^{-2} for the ZnCdSe QW laser emitting at the same wavelength. The temperature dependences of the threshold power density for the both lasers are nonmonotonic, with minima at 100 and 70 K, respectively, which is, probably, explained by different values of the energy gap between the lh and hh minibands responsible for the thermally activated vertical transport of holes in the SL waveguide. In addition, the CdSe FM laser showed no degradation after 24 hours for an excitation power density exceeding the threshold density (~ 100 kW cm^{-2}) by a factor of twenty-five, whereas the QW laser degraded after an hour for $P \sim 5P_{thresh}$. We assume that the record low values of P_{thresh} and improved degradation stability of optically pumped lasers are caused by the efficient localization of charge carriers in CdSe-enriched nanoislands, which prevents their migration towards larger relaxed islands and other defect regions where they could recombine nonradiatively, stimulating the multiplication of defects in the active region [21, 22].

CW BeMgZnSe laser diodes containing an SL waveguide, a single 2.6-ML CdSe FM recombination region, and operating at 300 K were manufactured for the first time. These lasers exhibit a blue shift of the lasing wavelength with time, which is accompanied by an approximately twofold increase in the threshold current density. One can assume that this phenomenon, which was not observed in the ZnCdSe QW structure, is caused by gradual degradation of large, close to critical size, islands with deeper lying levels.

Conclusions

The results of studies of blue-green DHS lasers based on the (Zn, Mg) (S, Se) and (Be, Mg, Zn)Se compounds grown by MBE are presented. To increase the degradation stability of lasers, a new concept for the active region design is suggested and realized. The new laser design contains a modified waveguide based on alternately strained short-period SL (of the type ZnSSe/ZnCdSe or BeZnSe/ZnCdSe), which protects the active region from penetration of structural defects, and the CdSe FM recombination region of thickness 2 – 3 MLs, which can transform, under certain MBE conditions, to a dense array of self-organizing pseudomorphic CdSe-enriched islands with lateral dimensions 15 – 30 nm, which serve as efficient centers for localization of charge carriers, producing spatial separation of the defects and radiative recombination regions. A substantial increase in the electronic and optical confinement, and quantum efficiency, as well as the efficient transport of charge carriers through the SL waveguide resulted in a record low threshold power density (less than 4 kW cm^{-2} at 300 K) in (Zn, Mg) (S, Se) lasers with a CdSe FM active region. (Be, Mg, Zn)Se/ZnCdSe SL QW heterostructure lasers possess the highest characteristic temperature ($T_0 = 340$ K at 300 K) and operating temperature (140°C) in the pulsed mode among those reported in the literature. All the lasers with a CdSe FM active region and SL waveguide exhibited enhanced degradation stability compared to conventional DHS SC QW lasers.

Acknowledgements
The authors thank H- J Lugauer, A Waag, and G Landwehr (Würzburg University, Germany) for fruitful cooperation in the MBE growth and studies of laser structures based on Be halcogenides. The authors also thank A A Sitnikova, R M Zolotareva, and S M Konnikov for TEM studies. This work was supported by grants of the Russian Foundation for Basic Research, the program "Physics of Solid-State Nanostructures" of the Russian Ministry of Science, and the Volkswagen Foundation.

References

1. Kato E et al. *Electron. Lett.* **34** 282 (1998)
2. Nakano K, in *Proc. 2nd Int. Symp. Blue Laser and Light Emitting Diodes, Chiba, 1998* p. 395
3. Verie C *J. Electron. Mater.* **27** 782 (1998)
4. Waag A et al. *J. Cryst. Growth* **184/185** 1 (1998)
5. Ivanov S V et al. *J. Cryst. Growth* **159** 16 (1996)
6. Ivanov S V et al. *J. Cryst. Growth* **184/185** 70 (1998)
7. Waag A et al. *Appl. Phys. Lett.* **70** 1 (1997)
8. Ivanov S V et al. *J. Appl. Phys.* **83** 3168 (1998)
9. Ivanov S V et al. *Appl. Phys. Lett.* **73** 2104 (1998)
10. Shubina T V et al. *J. Cryst. Growth* **184/185** 596 (1998)
11. Ivanov S V et al. *Semicond.* **32** 1137 (1998)
12. Toropov A A et al., in *Proc. Int. Symp. "Nanostructures: Physics and Technology"* (St. Petersburg, Russia, 1997) p. 210
13. Alferov Zh I et al. *Pis'ma Zh. Tekh. Fiz.* **14** 1803 (1988) [*Sov. Tech. Phys. Lett.* **14** 782 (1988)]
14. Lebedev A et al. *Acta Phys. Pol. A* **94** 421 (1998)
15. Toropov A et al., in *Proc. 2nd Int. Symp. Blue Laser and Light Emitting Diodes* (Eds K Onabe et al.) (Chiba, Japan, 1998) p. 254
16. Legge M et al., in *Proc. 2nd Int. Symp. Blue Laser and Light Emitting Diodes* (Eds K Onabe et al.) (Chiba, Japan, 1998) p. 409
17. Toropov A A et al., in *Proc. Inter. Symp. QD's, 1998, Sapporo, Japan* (to be published in *Jpn. J. Appl. Phys.*)
18. Toropov A A et al. *J. Cryst. Growth* **184/185** 293 (1998)
19. Sedova I et al. *Acta Phys. Pol. A* **94** 519 (1998)
20. Shubina T et al., in *Proc. 24th ICPS* (Jerusalem, Israel, 1998) p. Mo – P33
21. Ivanov S V et al., in *Proc. 2nd Int. Symp. Blue Laser and Light Emitting Diodes* (Eds K Onabe et al.) (Chiba, Japan, 1998) p. 419
22. Ivanov S V et al. *Appl. Phys. Lett.* **74** 498 (1998)

PACS number: 73.23.Hb

One-electron transistors based on Coulomb blockade and quantum interference

Z D Kvon, L V Litvin, V A Tkachenko, A L Aseev

The subject of the report are two limiting cases of 'one-electronics'. In the first part, we present the results of the development and study of a type of transistor based on Coulomb blockade, and in the second part, we discuss the concept of a one-electron interference transistor and the first experiments with it.

Transistor based on Coulomb blockade

The basic part of the channel of all the transistors discussed below is a conductor with capacitance $C_{\rm g}$ that is low compared to the gate capacitance. When the conductor is isolated from the main circuit by tunneling barriers, the conductivity peaks correspond to the removal of the Coulomb blockade of tunneling $C_{\rm g}V_{\rm g} + q = (n + 1/2)e$, where n is an integer and q is the constant polarization charge of the Coulomb island [1]. Therefore, to switch the transistor to the neighboring open state, it is necessary to add an elementary charge $C_{\rm g}$ to the capacitance e. Because the necessary condition for operation of a transistor has the form $e^2/2(C_1 + C_2 + C_{\rm g}) \gg k_{\rm B}T$, the capacitances C_1 and C_2 of tunneling transitions should be made as low as possible. The use of a conventional method of shadow masks gives an operating temperature for the transistor of 0.2 K for a lithographic size of 100 nm, while to achieve $T = 4.2$ K, lithography with a resolution of 30 nm would be required. We overcame this difficulty by breaking a titanium nanowire with a rectangular projection, which was previously made on a dielectric substrate (Fig. 1a). Tunneling transitions with a small barrier height (~ 10 meV) were formed by oxidation of a thin titanium film at two 10-nm steps under conditions of oxygen deficiency. For a lithographic size of 150 nm, the capacitances of tunneling transitions decreased to $(10-30)\times10^{-18}$ F due to deviation from the flat condenser geometry. The geometry of the device was controlled by means of a transmission electron microscope with a resolution of several A; for this purpose, the structures were manufactured on thin membranes of silicon nitride on silicon. Figure 1c shows that the transistor exhibits distinct oscillations of the current as a function of the gate voltage at 4.2 K. In accordance with the theory [1] and numerical calculations [2], the peak-to-valley ratio for oscillations increases with decreasing pulling voltage. Thus, the one-electron charging of the Coulomb island and Coulomb blockade were clearly observed (Fig. 1b). Also, random switchings of the conductivity were observed, which corresponded to a change in the polarization charge of the Coulomb island by a few tenths of the elementary charge. Thus, it has been shown that the device operates as a one-electron transistor and its stability has been studied. Note that the rupture of nanowires by a step on the dielectric surface has already been used for manufacturing one-electron diodes, however, this is the first fabrication of a transistor by this method.

Interference two-electron oscillations

A one-electron transistor usually means a transistor based on Coulomb blockade. However, it can be easily shown that interference transistors based on one-dimensional Fermi systems also allow one to realize a mode of counting of electrons added to the active region of the device. Indeed, consider a quantum wire of length L, in which only one miniband of transverse quantization is filled. At zero temperature, the relation between the Fermi wave vector $k_{\rm F}$ and the electron concentration $N_{\rm w}$ has the simple form

$$k_{\rm F} = \frac{\pi}{2} N_{\rm w} \,. \tag{1}$$

The number of electrons in the wire is $N_L = N_{\rm w}L$. Taking into account Eqn (1), we obtain that a change in the number of